

Traffic excited vibrations acting on pedestrians using a highway bridge

Reto Cantieni

rci dynamics, Structural Dynamics Consultants, Duebendorf, Switzerland

ABSTRACT: Whereas the middle part of the 27 m wide Langensand Bridge is used by five traffic lanes, pedestrian and cyclist lanes are located on the two 6 m cantilevers. The questions to be answered were: Are the pedestrians walking on the bridge cantilevers annoyed by traffic induced vibrations? If yes, what would be the optimum layout for TMD's? The experimental investigation included an ambient modal test as well as 77 dynamic load tests with three heavy vehicles being driven over the bridge in different configurations. With the ambient modal test 21 natural bridge modes in the $f = 1 \dots 34$ Hz range could be identified. For the load tests, maximum acceleration amplitudes measured at the free cantilever end were in the range of $a = 0.5 \dots 0.8$ m/s². These values were rated as being acceptable. Four of the bridge natural modes identified would have been subject to damping measures.

1 INTRODUCTION

The Langensand Bridge is a single span steel/concrete composite bridge with a span length of 79.7 m and a width of 27.3 m (Fig. 1). The skewness of the abutment axes is 17°. Two steel box girders are connected to a concrete bridge deck (Fig. 2). There were two challenges with this bridge.

Firstly, the bridge had to be built in two parts. The bridge link being vital to Lucerne, it was not possible to completely stop traffic for a longer period of time. Therefore, replacement of the existing bridge was performed in four steps: a) demolition of half of the old bridge, b) construction of half of the new bridge in 2008 (Fig. 2), c) demolition of the remaining half of the old bridge, and d), construction of the second half of the new bridge in 2009 (Fig. 2).

Secondly, the structure had to bridge the 11 railway tracks underneath in one span instead of the two spans of the existing bridge.

The problem under discussion here becomes obvious from the cross section shown in Figure 2. There are five traffic lanes in the bridge center part and two pedestrian/cyclist lanes on each of the two about 6 m wide cantilevers. In the bridge design stage it was not possible to decide whether or not the users of the cantilever lanes would be annoyed through vibrations excited through vehicular traffic flowing in the five bridge center lanes. It was therefore decided to investigate into this problem with experimental methods. To avoid the risk of not being in a position to quickly respond to possible problems through installation of tuned mass dampers, the experiments were performed in two ways: a) identify the bridge natural dynamic characteristics, and, b) determine the traffic excited cantilever tip vibrations. In case of the cantilever vibrations being rated to being unacceptable, the information on the bridge mode shapes and damping coefficients necessary to design tuned mass dampers, TMD's, would be available without any further delay. The tests were performed some weeks prior to opening of the 2008 half of the bridge (Fig. 2).

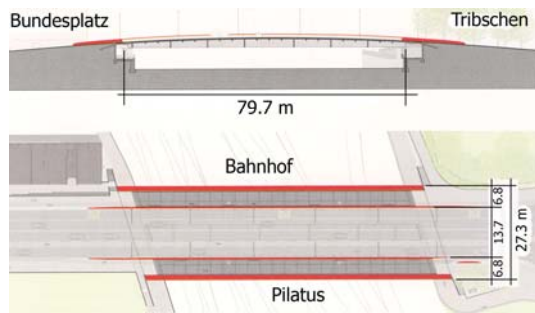


Figure 1: Langensand Bridge. Plan view.

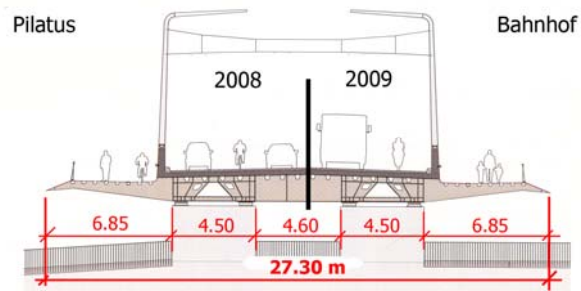


Figure 2: Langensand Bridge. Cross section. The paper covers tests performed on the Pilatus side half of the bridge (2008).

(Underlying graphics of both Figures: TU Bruno Zwahlen Mayr, courtesy tec21, the Journal of the Swiss Association for Civil Engineers and Architects.)

2 AMBIENT VIBRATION TESTS; INSTRUMENTATION

As no reliable data from an FE-analysis were available a pilot test was performed as a first step. As a result, the fundamental natural mode's frequency was identified to $f = 1.28$ Hz. This knowledge allowed optimum choice of the sensors to be used. Furthermore, the initially planned measurement point layout had to be revised. The pilot test, using two 3D measurement points at 0.4 of the span had revealed that the transverse as well as the longitudinal bridge vibrations were much more intense than assumed. Therefore, of the 52 measurement points, half were equipped with 1D, the other half with 3D acceleration sensors (Fig. 3).

Figures 4 and 5 show the arrangement of the measurement points and the respective DOF's. The two references chosen at 0.33 and 0.4 of the span length were 3D points. Another eight sensors were used to equip two 1D and two 3D rovers. As two remaining points could not be covered with this schedule, two additional 1D sensors were used in setups 1 and 2.

Sensors used:	PCB 393B31, 10 V/g, 3D version see Figure 3.
Frontend used:	LMS Pimento, 16 channels, 24 bit ADC, 14 or 15 channels used.
Sampling rate:	100 Hz.
Time window length per setup:	30 minutes.
Number of setups:	12
Total testing time:	8 hours.
Outdoor temp.:	plus 2 degrees C.



Figure 3: 3D measurement point.

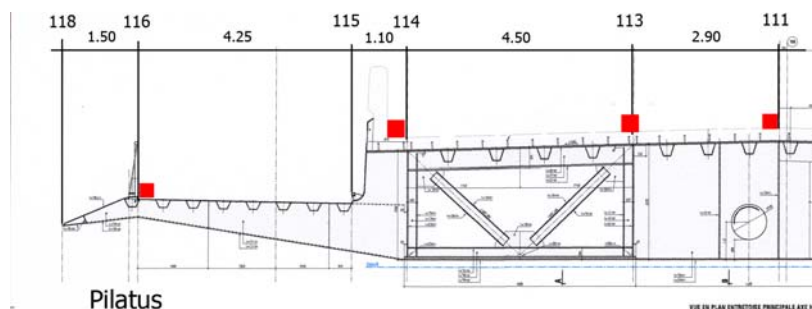


Figure 4: Ambient tests. Location of the four longitudinal measurement axes 111, 113, 114 and 116. Dimensions: meter.

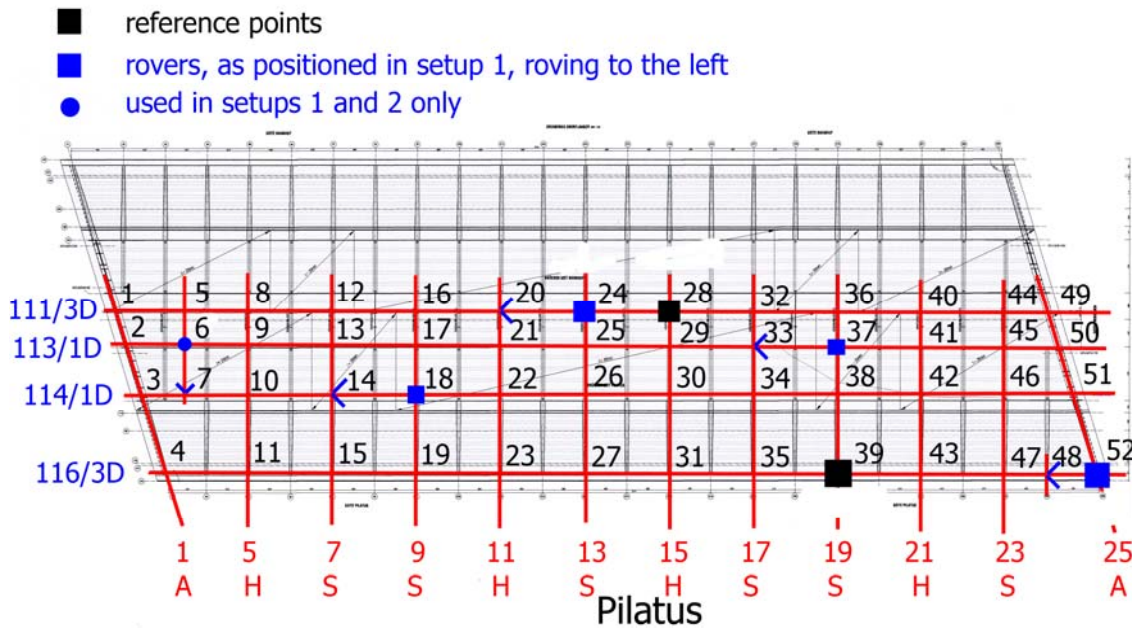


Figure 5: Ambient tests. Instrumentation layout.

3 AMBIENT VIBRATION TESTS; SIGNAL PROCESSING AND RESULTS

Applying the Artemis Software Suite and making use of the EFDD (Enhanced Frequency Domain Decomposition) routines allowed identification of 21 bridge modes in the frequency range $f = 1.27 \dots 34.04$ Hz. The SVD diagram presented in Figure 6 shows the number of projection channels having been chosen to 6. The number of frequency lines for $f = 0 \dots 50$ Hz was chosen to 1'024. Table 1 summarizes frequency, damping and schematic shape of the bridge first 17 natural modes.

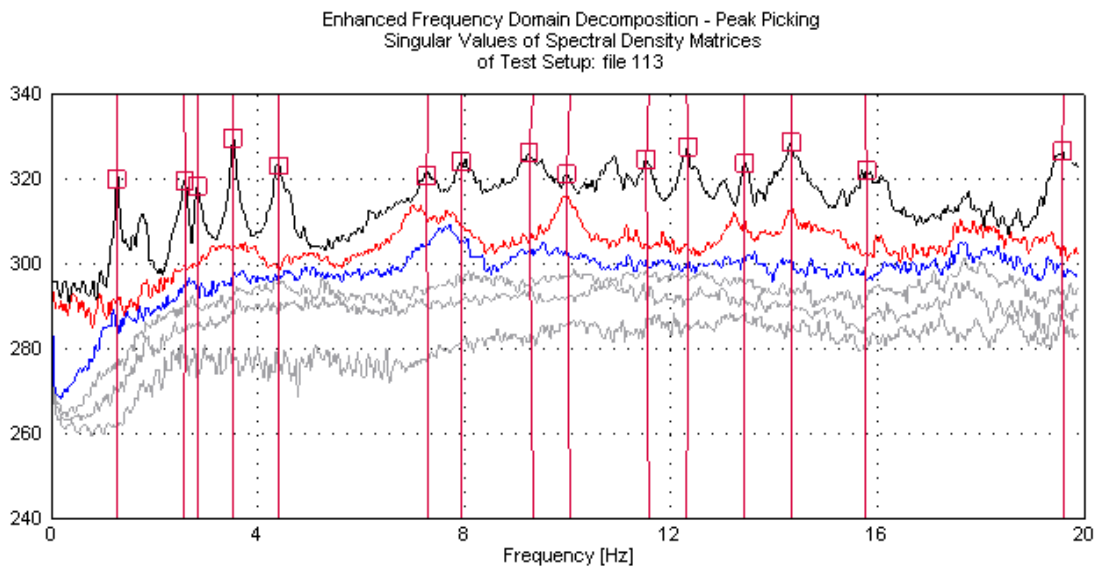


Figure 6: Ambient tests. EFDD-SVD diagram. For the sake of legibility this graphic covers the frequency range $f = 0 \dots 20$ Hz only.

Table 1: Ambient tests. Frequency, damping and schematic shape of the first 17 modes identified.
 $f < 10$ Hz: Global bridge modes, $f > 10$ Hz: "Local" cantilever modes.

	frequency [Hz]	damping [%]	type	
1	1.27	1.69	1. longitudinal bending	LB1
2	2.58	1.62	1a. transverse bending plus torsion	TB1a
3	2.82	1.38	1b. transverse bending plus torsion	TB1b
4	3.56	0.88	2. longitudinal bending	LB2
5	4.40	1.45	1. torsion plus 1. cantilever	TC1
6	7.29	1.80	3. long. bend. plus 2. transv. bend.	LB3TB2
7	7.95	1.25	2. cantilever	C2
8	9.34	1.74	2. torsion	T2
9	10.05	0.78	3. cantilever	C3
10	11.57	0.85	5a. cantilever Tribschen side	C5a
11	12.31	0.89	5b. cantilever Bundesplatz side	C5b
12	13.43	0.44	"strange" cantilever vibration	CS
13	14.35	0.63	7. cantilever	C7
14	15.75	0.70	8. cantilever	C8
15	19.61	0.69	10. cantilever	C10
16	21.71	0.79	11. cantilever	C11
17	23.69	0.87	12. cantilever	C12

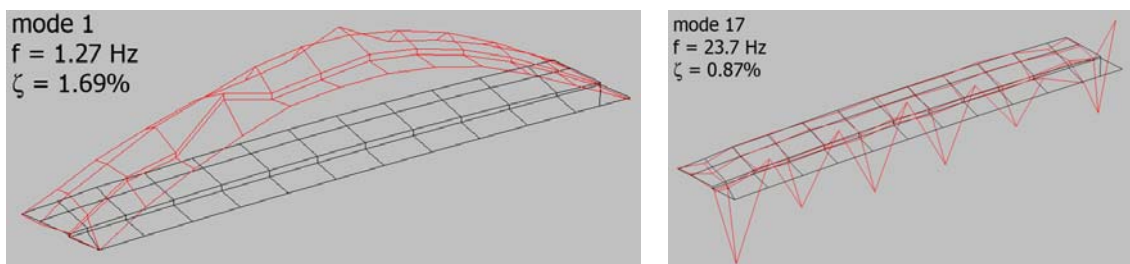


Figure 7: Modes No. 1 and No. 17 illustrating the bandwidth in frequency and shape of this bridge.

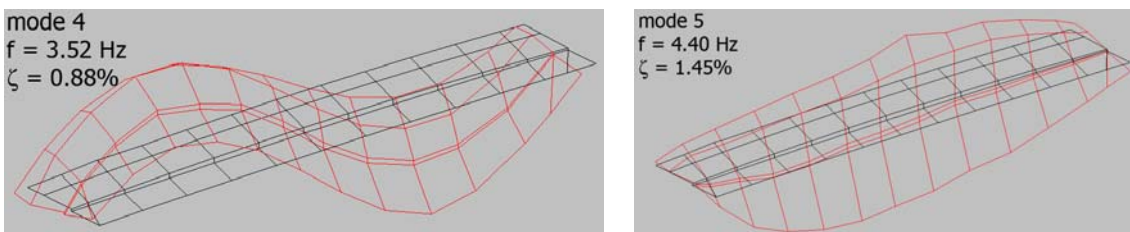


Figure 8: Bridge modes No. 4 and No. 5. These two modes proved to be decisive for the bridge vibrations excited through the heavy vehicles in the body bounce mode (see. Paragraphs 4 and 5).

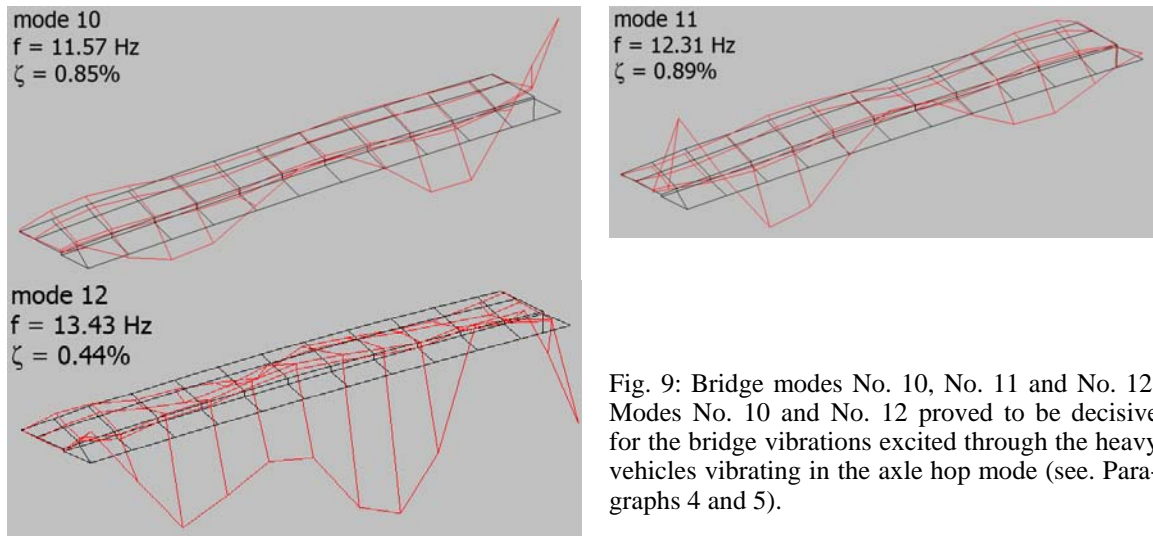


Fig. 9: Bridge modes No. 10, No. 11 and No. 12. Modes No. 10 and No. 12 proved to be decisive for the bridge vibrations excited through the heavy vehicles vibrating in the axle hop mode (see. Paragraphs 4 and 5).

4 VEHICLE EXCITATION

No reliable information on the bridge natural dynamic behavior was available before the tests. To make sure all possible resonance problems would be covered with the tests with heavy vehicles crossing the bridge, three vehicles with different suspension systems were used. The dynamic wheel load frequencies exerted by a heavy vehicle depend significantly on its suspension system.

Figure 10 shows an undamped quarter-car model to explain a vehicle's basic vibrational modes. The model has four elements: a) the body mass, b) the suspension spring, c) the unsprung mass, and, d) the tire spring. Since we are having a simple two-degree-of-freedom system here, this has two natural modes: a) the body bounce mode (in-phase), and b) the axle hop mode (out-of-phase). With the body bounce mode, the unsprung mass does not move compared to the large movement of the body mass. With the axle hop mode, the body mass does not move compared to the large axle movement. The modes are practically uncoupled (see the related frequencies given below). This is due to the facts that the body mass is much larger than the unsprung mass (the axle) and that the suspension spring is much softer than the tire spring.

The predominant dynamic wheel load frequencies are $f = 1.5 \dots 1.8$ Hz for air and $f = 2.5 \dots 3.5$ Hz for steel suspended vehicles in the body bounce mode and $f = 10 \dots 15$ Hz in the axle hop mode for both suspension systems (Cantieni et al 2000).

The test vehicles chosen were therefore a steel-suspended 4-axle 35-kN-Truck, an air-suspended 4-axle 35-kN-Truck and, because the bridge is also used by a Bus Service, a three-axle air-suspended 25-kN Bus (Figs. 11 to 13).

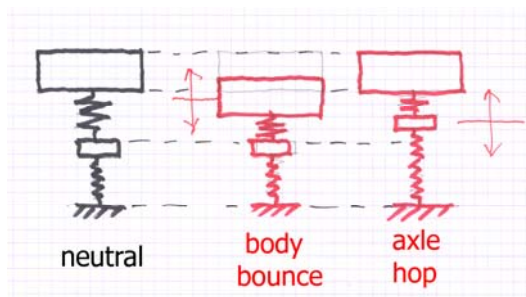


Figure 10: Quarter car model vibration modes.



Figure 11: The three test vehicles crossing the bridge.



Figure 12: Rear axle steel suspension.



Figure 13: Rear axle air suspension.

5 DYNAMIC LOAD TESTS WITH VEHICLES CROSSING THE BRIDGE

A total of 77 passages were performed with varying the vehicle speed (5 to 40 km/h), the number of vehicles (1, 2 or 3) the driving lane and the pavement roughness (without and with a 25 and 50 mm plank respectively at mid-span). Figures 14 and 15 give the layout of the three cantilever measurement points and the situation concerning the two traffic lanes used. From the three acceleration directions measured the vertical component was determining and is discussed here only.

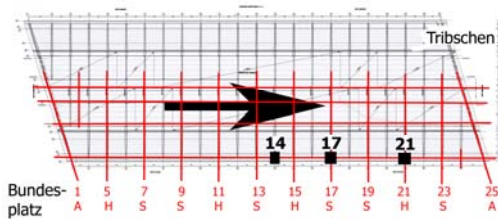


Figure 14: Location of the three 3D measurement points MP 14, MP 17 and MP 21. The driving direction is indicated.

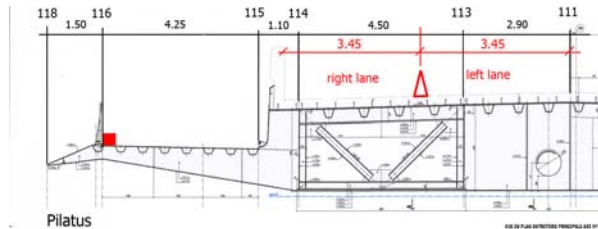


Figure 15: Location of the measurement points in the cross section (red square); situation of the two driving lanes.

Table 2: Dynamic load tests. Maximum vertical acceleration measured.

	MP 14 amax [m/s ²]	MP 14 who	MP 17 amax [m/s ²]	MP 17 who	MP 21 amax [m/s ²]	MP 21 who
left lane no plank	0.60	air 35 km/h	0.79	air 40 km/h	0.75	air 35 km/h
right lane no plank	0.44	air + bus 25 km/h	0.50	air + bus 25 km/h	0.56	bus 30 km/h
	MP 14 amax	MP 14 who	MP 17 amax	MP 17 who	MP 21 amax	MP 21 who
left lane 25 mm pl.	2.55	air+steel+bus 20 km/h	2.27	air+steel+bus 20 km/h	2.36	air+steel+bus 20 km/h
right lane 25 mm pl.	1.31	air + bus 20 km/h	1.20	air + bus 20 km/h	0.82	air+steel+bus 20 km/h
left lane 50 mm pl.	2.50	steel 20 km/h	2.63	air+steel+bus 10 km/h	2.54	air + bus 20 km/h
right lane 50 mm pl.	1.69	air + bus 20 km/h	1.38	air + bus 20 km/h	1.35	air + bus 20 km/h

6 ACCEPTANCE OF CANTILEVER VIBRATION LEVELS

There are many references dealing with the question of allowable vibration levels induced into pedestrians on bridges. Two of them are cited in the references (Bachmann ed. 1995) (Bachmann and Ammann 1987). Human beings tend to have different levels of acceptance versus vibrations. It is therefore not possible to define a given number as a firm limit. The tendency in the literature is that vibrations with $a_{max} = 0.5 \text{ m/s}^2$ are not likely to result in complaints and that this may change for vibrations with a_{max} larger than $a_{max} = 1.0 \text{ m/s}^2$. For passages without a plank, the value of $a_{max} = 0.8 \text{ m/s}^2$ has not been surpassed for the new Langensand Bridge Pilatus Half. The owner therefore decided to leave the bridge without TMD's and respond to complaints as they arrive.

7 BRIDGE VEHICLE INTERACTION

The main purpose of the ambient structural identification test discussed at the beginning was to dispose of the necessary information to allow designing TMD's without further delay in case of the vibration levels induced by the heavy vehicles not being acceptable. The measured time signals were therefore analyzed in detail in the frequency domain. The bridge natural frequencies were known quite well, of course with some flexibility due to the vehicles mass effect on these.

Inspection of the cantilever tip vibration frequency spectra yielded that four bridge natural modes are predominantly responsible for the dynamic bridge response at the cantilever tip Pilatus side. This does not include the first bridge mode where the shape would have been optimum but the frequency is too low.

- f4, LB2, $f = 3.52 \text{ Hz}$, second main girder longitudinal bending mode (Fig. 8),
- f5, TC1, $f = 4.40 \text{ Hz}$, first main girder torsion and first cantilever bending (Fig. 8),
- f10, C5a, $f = 11.6 \text{ Hz}$, 5th cantilever bendig Tribschen side (Fig. 9),
- f12, CS, $f = 13.4 \text{ Hz}$, "strange" cantilever vibrational shape (Fig. 9).

The results being quite complex it is not possible to discuss them in detail here. It is however attempted to illustrate the dynamic cantilever tip behavior as a function of the test parameters.

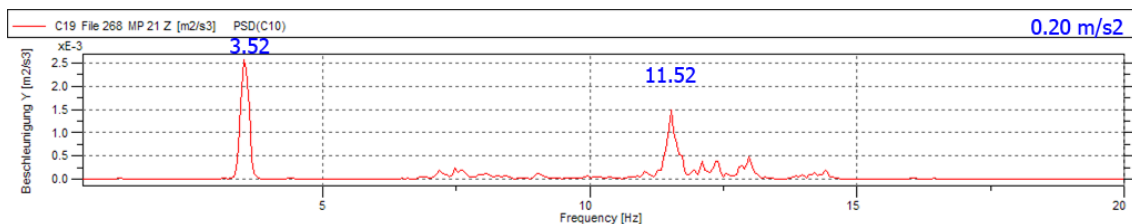


Figure 16: MP 21, Air suspended vehicle, right lane, 20 km/h. Right lane means: driving on the box girder. Global modes without a node in MP 21 (3.52 Hz) are more likely to be excited than local cantilever modes (11.57 Hz). The maximum amplitude (indicated in the graphic's top right hand corner) is comparatively small (0.2 m/s²).

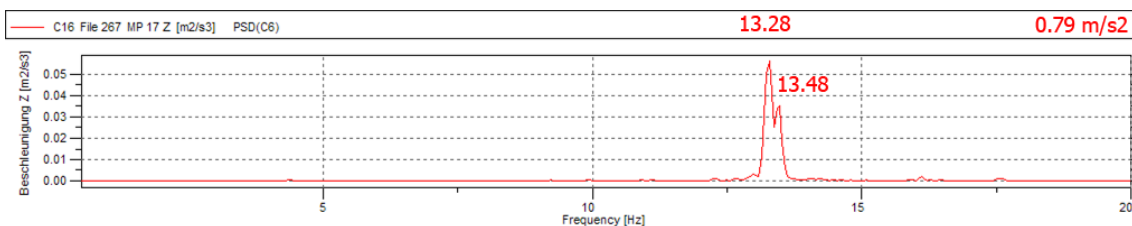


Figure 17: MP 17, Air suspended vehicle, left lane, 40 km/h. Driving in the left lane at a relatively high speed results in a nice excitation of cantilever mode No. 12. Although the modal amplitude in the driving lane is quite small, coincidence with frequency and the low modal damping lead to a maximum acceleration level in MP 17 where the modal amplitude is maximum.

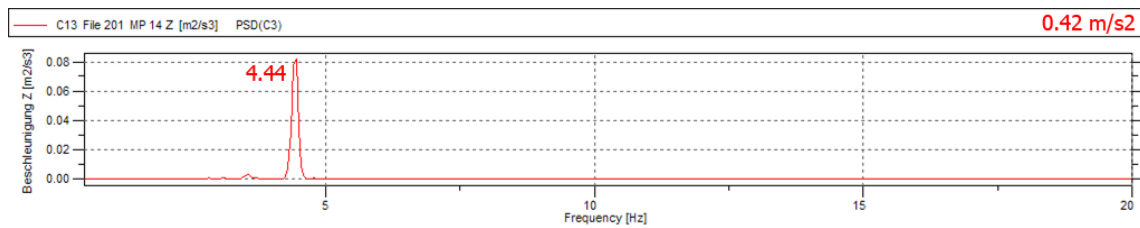


Figure 18: MP 14, Steel suspended vehicle, left lane, 20 km/h. The pavement being smooth, the steel suspended vehicle is generally less active in the axle hop mode than the vehicle with air suspension. The leaf spring being locked the vehicle vibrates on its tires only. There are two reasons for mode No. 5 (4.4 Hz) being excited instead of mode No. 4 (3.52 Hz) as shown in Figure 16: Mode No. 4 exhibits a node in MP 14 and Mode No. 5 is easier excited than Mode No. 4 for driving in the left lane than in the right lane (Fig. 8). The acceleration amplitude is quite high.

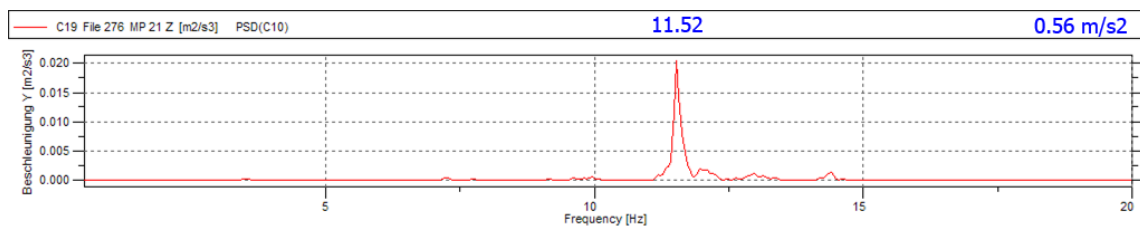


Figure 19: MP 21, Bus, right lane, 20 km/h. The shock absorbers in this suspension are probably quite worn. This results in the Bus exerting almost pure axle hop vibrations and exciting the cantilever at this quite high frequency even for using the right lane and at a comparatively low speed. The acceleration amplitude is quite high.

8 CONCLUSIONS

Identification of the Langensand Bridge natural modes and comparison with the frequency spectra of the traffic excited cantilever tip vibrations yielded that four of the 21 bridge modes are excited through traffic. Due to its low frequency the bridge fundamental mode with $f = 1.28$ Hz is not included. As a result of the bridge superstructure being half wing-shaped and half beam-shaped and of the resulting unusual mode shape variety and complexity the dynamic cantilever tip behavior strongly depends on the position of the driving axis, the vehicle suspension system and the location of the response measurement point. The cantilever tip vibrations excited through the passage of heavy vehicles are quite important. The respective intensity can be supposed to increase with decreasing pavement evenness. Designing a TMD system to reduce the cantilever vibrations would be quite challenging: Today, four bridge modes with frequencies in the $f = 3.5 \dots 13.5$ Hz region and exhibiting quite complex shapes should then be acted upon. And there are more modes waiting to be excited with changing excitation parameters.

9 REFERENCES

- Cantieni, R., Krebs, W., Heywood, R., 2000. *OECD IR6 DIVINE Project, Dynamic Interaction Between Vehicle and Infrastructure Experiment, Element 6, Bridge Research, Final Report*. EMPA Test Report No. 153'031, Duebendorf.
- Bachmann, H., ed., 1995. *Vibration Problems in Structures – Practical Guidelines*. Birkhaeuser Verlag Basel, Boston, Berlin, ISBN 3-7643-5148-9.
- Bachmann, H., Ammann, W., 1987. *Schwingungsprobleme bei Bauwerken*. Structural Engineering Documents 3d. IABSE, International Association for Bridge and Structural Engineering, Zurich. (Published in English as IABSE Structural Engineering Documents 3e).